

Received April 15, 2019, accepted May 6, 2019, date of publication May 15, 2019, date of current version May 24, 2019.

Digital Object Identifier 10.1109/ACCESS.2019.2916934

A Fast Fractal Based Compression for MRI Images

SHUAI LIU^{ID1}, WEILING BAI², NIANYIN ZENG^{ID3}, AND SHUIHUA WANG^{ID4}

¹Hunan Provincial Key Laboratory of Intelligent Computing and Language Information Processing, College of Information Science and Engineering, Hunan Normal University, Changsha 410000, China

²College of Computer Science, Inner Mongolia University, Hohhot 010010, China

³Department of Instrumental and Electrical Engineering, Xiamen University, Xiamen 361000, China

⁴School of Architecture Building and Civil Engineering, Loughborough University, Loughborough LE11 3TU, U.K.

Corresponding authors: Nianyin Zeng (zny@xmu.edu.cn) and Shuihua Wang (shuihuawang@ieee.org)

This work was supported in part by the National Natural Science Foundation of China under Grant 61502254, in part by the Program for Yong Talents of Science and Technology in Universities of Inner Mongolia Autonomous Region under Grant NJYT-18-B10, in part by the Open Project Program of the State Key Lab of CAD&CG under Grant A1926, Zhejiang University, and in part by the Open Project Program of the State Key Laboratory of Complex Electromagnetic Environment Effects on Electronics and Information System under Grant 2019K0104B.

ABSTRACT Magnetic resonance imaging (MRI), which assists doctors in determining clinical staging and expected surgical range, has high medical value. A large number of MRI images require a large amount of storage space and the transmission bandwidth of the PACS system in offline storage and remote diagnosis. Therefore, high-quality compression of MRI images is very research-oriented. Current compression methods for MRI images with high compression ratio cause loss of information on lesions, leading to misdiagnosis; compression methods for MRI images with low compression ratio does not achieve the desired effect. Therefore, a fast fractal-based compression algorithm for MRI images is proposed in this paper. First, three-dimensional (3D) MRI images are converted into a two-dimensional (2D) image sequence, which facilitates the image sequence based on the fractal compression method. Then, range and domain blocks are classified according to the inherent spatiotemporal similarity of 3D objects. By using self-similarity, the number of blocks in the matching pool is reduced to improve the matching speed of the proposed method. Finally, a residual compensation mechanism is introduced to achieve compression of MRI images with high decompression quality. The experimental results show that compression speed is improved by 2–3 times, and the PSNR is improved by nearly 10. It indicates the proposed algorithm is effective and solves the contradiction between high compression ratio and high quality of MRI medical images.

INDEX TERMS MRI, image compression, fractal compression, spatiotemporal similarity, lossy compression.

I. INTRODUCTION

Medical imaging has become one of the most active and rapidly evolving fields in medical research and clinical diagnosis. Medical images display the internal structure of the human body in an intuitive form, providing clinicians with intuitive and accurate basic information on anatomy, pathology and function. Typical imaging modalities include magnetic resonance imaging (MRI), computer-assisted tomography (CT), ultrasound (US), computer-assisted X-ray (CR), digital subtraction angiography (DSA), et al. With continuous advancement of medical imaging technology, especially the resolution of imaging devices, the amount of medical image data will continue to grow. Existing bandwidth

conditions are difficult to meet the real-time transmission requirements of large data volumes. To meet effective storage and transmission of medical images, it is not only necessary to expand storage space and transmission bandwidth, but also to study how to efficiently compress medical data. Therefore, it is necessary to implement effective compression of various medical images using an image compression algorithm.

Medical image compression methods are generally classified into lossless compression and lossy compression. Lossless compression provides medical diagnostics with image information of the same quality as the original image. However, the compression ratio of lossless compression is usually low, which is difficult to meet the actual transmission requirements of medical images. Lossy compression provides a higher compression ratio by losing some information. Increase in compression inevitably brings a certain degree of

The associate editor coordinating the review of this manuscript and approving it for publication was Yudong Zhang.

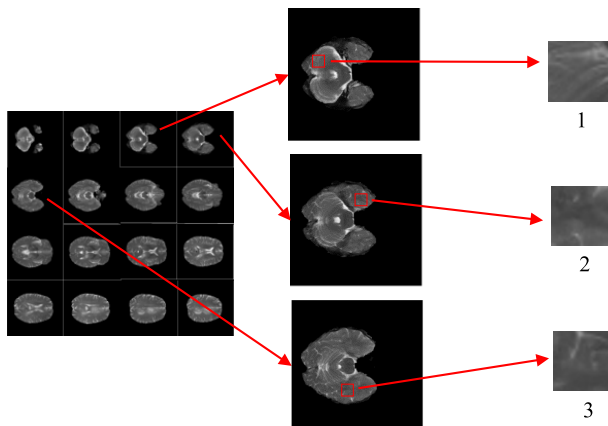


FIGURE 1. Spatiotemporal correlation of MRI medical images.

degradation to medical images. In the future of telemedicine applications, lossless compression will be difficult to provide a low bit rate required for image transmission, while relying on lossy compression to achieve real-time transmission of images. At present, lossy compression technology for medical images has become a research hotspot at domestic and international, and its research goal is to improve the reconstruction quality of images as much as possible under a given code rate.

MRI medical images contain rich temporal and spatial correlations. As shown in Fig. 1, three similar image blocks 1, 2, and 3 are respectively derived from three adjacent MRI medical image slices. The spatiotemporal correlation means that in a MRI image slice, its adjacent fields of a certain pixel (region) in a layer of image (several layers before and after) have a strong similar relationship with the pixel (region). This spatiotemporal correlation makes a large amount of (local) self-similar information contained in MRI images. Therefore, it is considered to compress this type of medical image using the fractal compression idea. Fractal image compression is based on Iterated Function System (IFS), omitting the image content, and only retaining self-similarity parameters of the local image content to complete data compression. It has advantages of high compression ratio, reconstruction at any scale, and fast decoding. However, traditional fractal compression algorithm fails to fully consider the spatiotemporal relationship of MRI images, resulting in inefficient and poor results. Therefore, a fast fractal-based compression algorithm for MRI images is proposed in this paper.

In this study, our contribution is to apply sequence image-based fractal compression method to compress three-dimensional MRI images. Besides, to get better performance of compression, we proposed two improvements. First, range blocks and domain blocks are classified according to the spatiotemporal similarity feature. A range block only needs to search for the optimal matching block in a certain type of domain block. Compression process is accelerated by reducing the capacity of matching pool. Second, the residual compensation mechanism is introduced to achieve

approximate lossless compression of MRI images. The experimental results show that the proposed method improves compression efficiency under the premise of ensuring image quality of MRI.

The rest of this paper is organized as follows. In Section 2, we review the progress of medical image compression research from both ROI coding and non-ROI coding. Section 3 elaborates on a fast fractal-based compression method for MRI image. In Section 4, we verify feasibility of the proposed method through experiments. Finally, Section 5 summarizes our work and describes future research directions.

II. RELATED WORKS

Under application conditions such as telemedicine, the compression ratio of lossless compression is difficult to meet transmission requirements for real-time images. It is necessary to resort to a lossy compression method. At the expense of image portion information, a target bit rate required for real-time transmission is exchanged. Selective image compression technology is gaining an increasingly important role in telemedicine or medical imaging applications with large storage needs. Its production effectively alleviates the contradiction between high compression ratio and lossless compression of medical images. The compression method based on region of interest (ROI) has become an important selective image compression technology, which accounts for a large proportion in published literatures. This paper will review the research progress of medical image compression from both ROI coding and non-ROI coding.

A. ROI CODING

Medical image compression algorithm based on ROI coding first divides an image into ROI and background (BG), wherein the ROI region usually adopts lossless or near lossless compression, and the BG region usually performs a large degree of lossy compression. Bruckmann and Uhl [1] compared the performance of lossy compression based on wavelet transform and JPEG in selective image compression techniques. Experimental results show that the selective compression performance of wavelet transform was better than JPEG. Based on the ROI coding provided by JPEG2000, Tahoces *et al.* [2] proposed a selective coefficient mask displacement coding algorithm. The wavelet coefficients belonging to different sub-bands were shifted to implement ROI coding. Zhang *et al.* [3] proposed a classification method based on neural network. Hosseini and Naghsh-Nilchi [4] proposed context-based vector quantization (CVQ) algorithm to achieve high-fidelity compression of medical ultrasound images. The algorithm used the region growing method to separate ROI and BG in an image, and then used the proposed CVQ scheme to compress the two parts separately. In the algorithm proposed by Sophia and Anitha [5], the ROI part of an image is losslessly compressed by run-length coding, Huffman coding or arithmetic coding, and the BG part is subjected to lossy compression based on vector quantization.

The algorithm proposed by Kaura and Wasson [6] used the fractal algorithm to perform lossy compression on BG, and performs lossless compression based on context tree weighting (CTW) on ROI.

Lesions in medical images and other infected sites have a more important diagnostic significance than the overall image. Schelkens *et al.* [7] combined the embedded zerotree wavelet (EZW) coding algorithm with the multi-ROI general protocol to improve scalability of the embedded code stream. Sridhar [8] proposed a dual ROI coding algorithm for medical images in which the lesion area was considered to be the ROI, and the surrounding lesion (usually susceptible area) was the secondary ROI, giving the two ROIs different levels of priority. Hu *et al.* [9] proposed a multi-ROI medical image compression algorithm based on edge feature protection. The algorithm used the Canny operator to extract useful image edge information, combined JPEG2000 to reduce the ROI losslessly, and used a multi-level tree set split in hierarchical tree (SPIHT) to compress the BG. For vascular images, Firoozbakht *et al.* [10] proposed a compression algorithm based on context and multi-ROI coding. The algorithm divided a vascular image into a primary ROI (vascular stenosis region), a secondary ROI (other important areas of blood vessels), and BG. The main ROI usually needed to be manually selected, while the secondary ROI was automatically detected by the regional growth method. The component priority-based ROI coding method proposed by Bartrina-Rapesta *et al.* [11] utilized the optimal rate distortion technique and combined a simple and effective ROI code rate allocation strategy to achieve coding of multiple ROIs at different priorities.

For stereoscopic medical images, multidimensional wavelet transforms are typically used to remove correlations in various directions in the image. Agrafiotis *et al.* [12] extended 3D SPIHT algorithm to enable three-dimensional ROI coding. Wang and Cuhadar [13] proposed the use of unbalanced three-dimensional tree structure to achieve three-dimensional ROI coding of medical images, and achieved multi-ROI and multi-quality control. Victor *et al.* [14] proposed an improved three-dimensional scalable compression algorithm for medical images based on the optimal volume of interest (VOI) coding. Nguyen *et al.* [15] proposed an efficient compression algorithm using hierarchical vector quantization and motion compensation. The algorithm used three-dimensional motion estimation to create uniform pre-processed data, and used a three-dimensional compression algorithm based on hierarchical vector quantization to compress the pre-processed data. Sanchez [16] proposed a lossy compression algorithm for medical images based on multiple 3D ROI. The use of joint source channel coding enabled multiple three-dimensional ROIs to achieve higher transmission priorities in the context of wireless transmission. Sid Ahmed *et al.* [17] proposed an embedded image encoder based on efficient reversible discrete cosine transform (RDCT). The proposed rearrangement structure was well coupled to a lossless embedded zerotree

wavelet encoder (LEZW). The background was compressed using a set partitioning algorithm in hierarchical tree (SPIHT) technology. Yee *et al.* [18] applied a lossless BPG compression algorithm to the ROI region and a lossy BPG for the non-ROI region.

B. NON-ROI CODING

Sridhar and Prasad [19] combined the integer DCT-based SPIHT algorithm with context adaptive variable length coding (CAVLC) to encode important coefficients of medical images. Then, only these important coefficients were transmitted instead of transmitting the entire image data, thereby achieving compression effect. Based on the curled DCT (Warped DCT, WDCT), Prabhu *et al.* [20] proposed a 3D warped DCT (3D WDCT), by means of which a complete medical image compression scheme was presented. Bhavani and Thanushkodi [21] compared the performance of several fractal coding algorithms on MRI compression, including fractal coding standards, quasi-lossless fractal coding, and improved quasi-lossless fractal coding. Based on this, a novel quasi-lossless fractal compression algorithm was proposed, which effectively retained important features in the image. A machine learning method was used to reduce encoding time of the algorithm and improve compression performance. Juliet *et al.* [22] proposed a medical image compression algorithm based on Ripple transform, which introduced an anisotropic Ripple transform to represent singular points on an arbitrary shape curve, and encoded its important coefficients by SPIHT algorithm. Automatic and accurate classification of MRI images is important for the analysis and interpretation of these images. Zhang *et al.* [23] combined two successful techniques: pseudo Zernike moment and kernel support vector machine to pathological brain detection. This approach performed better than eleven state-of-the-art smart pathological brain detection methods in three open datasets.

In addition, Juliet *et al.* [24] proposed using sparse representation to explore the geometrical rules of image structure, and based on this, proposed a medical image compression algorithm. Geometric flow indicated the direction in which the gray level of the image changed regularly. The image was further refined along the direction of geometric flow by Bandelet transform. Bandelet coefficients were encoded by SPIHT algorithm, and then the global thresholding process combined with fixed coding was performed. Selvi and Nadarajan [25] proposed a fast compression method for four-dimensional fMRI images. The method utilized data recombination, Contourlet transform, and improved binary array technology. The test results for fMRI showed that performance of the algorithm was better than SPIHT or SPECK, and had lower complexity. Zhang *et al.* [26] proposed an MRI image classifier based on Particle Swarm Optimization and kernel support vector machine. Juliet *et al.* [27] proposed a projection-based medical image compression algorithm. Discrete radon transform (DRT) was used to effectively represent direction information of the image, and RANHT was used

to encode Randon transform coefficients. The test results for MRI and CT showed that compression performance of this algorithm was better than other types of SPIHT algorithms.

Patbhaje *et al.* [28] proposed a medical image compression technique based on adaptive scanning wavelet differential reduction (ASWDR). ASWDR technology utilized different wavelet filters and achieved different compression efficiencies based on unique sparse characteristics. Selvi and Nadarajan [29] proposed a fast two-dimensional lossy compression technique using wavelet-based contourlet transform (WBCT) and binary array technique (BAT) for computed tomography (CT) and magnetic resonance imaging (MRI) images. Pathak *et al.* [30] analyzed various prediction methods using spatial correlation properties of neighborhood pixels to minimize prediction errors. Experimental results showed that the support prediction method improved compression ratio and maintained marginal PSNR and minimum absolute error. The new method proposed by Amri *et al.* [31] combined image reduction and extension techniques, digital watermarking and lossless compression standards such as JPEG-LS (JLS) and TIFF formats. Zhang *et al.* [32] developed a novel machine learning system that automatically diagnoses Alzheimer's disease from MRI images. Parikh *et al.* [33] established an acceptable HEVC compression range for medical imaging applications based on established medically acceptable JPEG 2000 compression ranges. The complexity of diagnostically acceptable lossy compression and high depth medical image compression was investigated.

From the above review to research progress of medical image compression, it can be seen that the ROI-based compression method has received extensive attention and has a large proportion in published literatures. Purpose of introducing ROI coding is to protect some of the information useful for subsequent medical diagnosis under limited transmission bandwidth conditions. Transform-based method has been widely used in medical image compression. The currently used transformation method is still DWT. The adoption or design of more advanced transformation methods is expected to further improve compression performance. The proposed method improves compression speed of MRI images while ensuring image quality. Experimental results show the effectiveness of this method.

III. FAST FRACTAL-BASED COMPRESSION METHOD FOR MRI IMAGES

A. FRACTAL MRI IMAGE COMPRESSION BASED ON SEQUENCE IMAGE

Three-dimensional MRI image is essentially a data cube that adds third-dimensional information to a common two-dimensional image. For the form in which three-dimensional image has a data cube, we convert three-dimensional MRI image into two-dimensional sequence images for compression. First, the image to be compressed is divided into a series of fixed size $N \times N$ pixel sub-blocks. They do not overlap each other and cover the entire image, which is called a range block (R block). Subsequently, the image to be encoded is

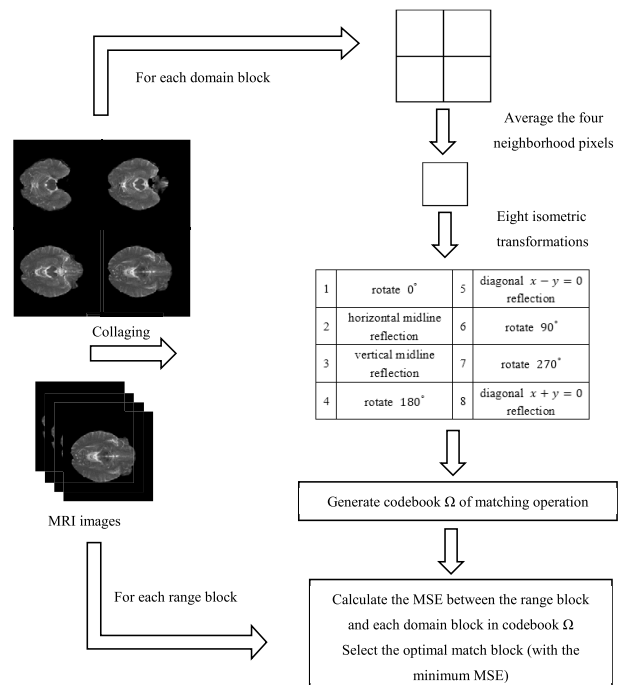


FIGURE 2. Flow chart of fractal MRI image compression based on sequence image.

again divided into domain blocks (D blocks) having a size of $2N \times 2N$, and D blocks may overlap. Before the encoding, D block is averaged by the four neighboring pixels, and its size is reduced to be the same as the size of R block. The averaged sampled D block is subjected to eight kinds of equidistant transformations, and the transformed whole constitutes codebook Ω . For each R block, it is necessary to find its best matching D block in the codebook Ω . Each R block is then approximated by the luminance transform of its best matching block $D \in \Omega$, that is $R = s \bullet D + o \bullet 1$. Where 1 is a unit matrix of $N \times N$, and s, o are the contrast and brightness adjustment factors of D block, respectively. Fractal MRI image compression process based on sequence image is shown in Fig. 2.

The following are specific steps of fractal MRI image compression algorithm based on sequence image:

Input: MRI image F of size $M \times M$.

Output: Fractal encoded file dx, dy, t, s, o .

Step 1: Perform fixed block partitioning on MRI image F , and divide it into a range block (R block) whose size is $N \times N$ but does not overlap each other.

Step 2: The $2N \times 2N$ intercepting window is moved in horizontal and vertical directions of the image F by a step size δ , and the intercepted block after each movement constitutes a domain block (D block).

Step 3: Perform average sampling and eight equidistant transformations on all D blocks to form a codebook Ω .

Step 4: For an arbitrary range block R_i , find the best matching block D'_j that satisfies Eq.1 in codebook Ω .

$$d(R_i, W_i(D'_j)) = \min \|R_i - (s_i \cdot (t_k(D'_j)) + o_i)\|^2 \quad (1)$$

In Eq.1, D'_j is the domain block after average sampling. $t_k \in \{t_1, \dots, t_8\}$ are eight isometric transforms. s_i and o_i are contrast factor and luminance factor of gradation transformation, respectively, and are calculated according to Eqs.2-3. n is the total number of pixels, and r_p, d_p are the p -th pixel values of range block and domain block, respectively.

$$s = \frac{n \sum_{p=1}^n d_p r_p - \sum_{p=1}^n d_p \sum_{p=1}^n r_p}{n \sum_{p=1}^n d_p^2 - (\sum_{p=1}^n d_p)^2} \quad (2)$$

$$o = \frac{1}{n} \left[\sum_{p=1}^n r_p - s \sum_{p=1}^n d_p \right] \quad (3)$$

B. CLASSIFICATION OF MRI IMAGE SUB-BLOCKS

In traditional fractal MRI image compression algorithm, each range block needs to perform a global search on the entire codebook Ω to find the best matching block, which is the main reason for long compression time [34]. In order to effectively solve this problem, we classify image blocks according to the spatiotemporal similarity feature. It makes matching range of range block greatly reduced. Moreover, continuous m-layer MRI images are combine them into one large image matrix for overall compression. The 'codebook' is expanded from a single frame image to a number of consecutive frames. When matching a range block, it is no longer limited to a single frame. Make full use of the inter-frame correlation to expand the matching pool. Matching error is reduced and compression quality is improved.

First, set the number m of classes, and then set a set of threshold sequences $\{\sigma_i\}$, $i = 1, 2, \dots, \sigma_1 = 0$. Find the mean $D_A = (h_{A1}, h_{A2}, \dots, h_{A2^b})$ of gray-scale feature vectors for all remaining domain blocks (excluding the former $i-1$ class) as the initial cluster center of the i -th domain block in Eq.4, where b is the number of bits per pixel, n is the total number of pixels.

$$\begin{cases} h_{A1} = \frac{1}{n} (h_{11} + h_{21} + \dots + h_{n1}) \\ h_{A2} = \frac{1}{n} (h_{12} + h_{22} + \dots + h_{n2}) \\ \dots \\ h_{A2^b} = \frac{1}{n} (h_{12^b} + h_{22^b} + \dots + h_{n2^b}) \end{cases} \quad (4)$$

Secondly, domain block $D'_j = (h_{j1}, h_{j2}, \dots, h_{j2^b})$ is taken out one by one from domain block set $\{D'_1, D'_2, \dots, D'_n\}$. The distance to cluster center D_A is calculated according to Eq.5.

$$dis(D_A, D'_j) = [\sum_{k=1}^{2^b} (h_{Ak} - h_{jk})^2]/2^b \quad (5)$$

Again, let the initial threshold be σ_p (σ_p is the median of threshold sequence $\{\sigma_i\}$), and the i -th class domain block C_{Di} corresponds to the threshold $\sigma_{Di} = \sigma_p$. Then, the domain block whose distance is less than or equal to σ_{Di} is divided into the i -th class C_{Di} .

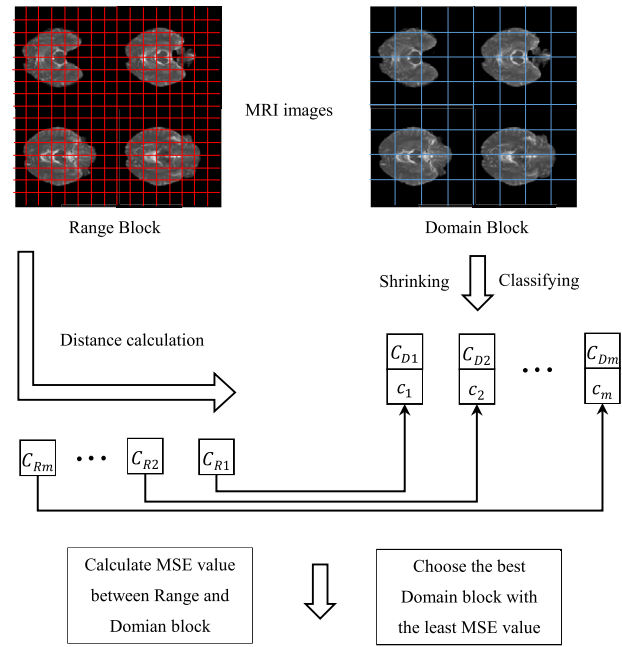


FIGURE 3. Flow chart of classified MRI image compression.

Suppose the class C_{Di} contains a number of domain blocks of ω_i . If $\omega_i \gg (\frac{M-2N}{\delta} + 1)^2/m$, the threshold is adjusted to $\sigma_{Di} = \sigma_{p-1}$, where σ_{p-1} is an order of magnitude smaller than σ_p . And so on until $|\omega_i - (\frac{M-2N}{\delta} + 1)^2/m| \leq 10^{(\log_{10} \omega_i - 1)}$ or $|\omega_i - \omega'_i| \geq 10^{(\log_{10} \omega_i - 1)}$.

Similarly, if $\omega_i \ll (\frac{M-2N}{\delta} + 1)^2/m$, the threshold σ_p is adjusted to σ_{p+1} . Until $|\omega_i - (\frac{M-2N}{\delta} + 1)^2/m| \leq 10^{(\log_{10} \omega_i - 1)}$ or $|\omega_i - \omega'_i| \geq 10^{(\log_{10} \omega_i - 1)}$. Adjustment of the threshold is stopped, and the i -th class domain block C_{Di} is determined.

Finally, m classes of domain blocks $C_{D1}, C_{D2} \dots C_{Dm}$ are obtained.

After getting domain block class, we also classify range blocks.

According to above steps of finding the initial cluster center, class centers $c_1, c_2 \dots c_m$ for m classes of domain blocks are obtained. Calculate the Euclidean distance between range block R_n and each class center $c_1, c_2 \dots c_m$, select the class with the smallest distance to perform a matching search, and obtain corresponding m class of range blocks $C_{R1}, C_{R2} \dots C_{Rm}$. In this way, each class of range blocks only needs to perform matching search in the same class of domain blocks, for example, the m -th range block class C_{Rm} and the m -th domain block class C_{Dm} is matched. The matching process between different classes of range blocks is performed independently. Reduction of matching range effectively reduces encoding time. The flow chart of MRI image compression in this paper is shown in Fig. 3.

The following are specific steps of classified MRI image compression algorithm in this paper:

Input: continuous m-layer MRI image $\{F_1, F_2, \dots, F_m\}$.
Output: Fractal encoded file dx, dy, t, s, o}.

Step 1: Take out continuous m-layer images $\{F_1, F_2, \dots, F_m\}$ in MRI image slices, and combine them into one large image matrix F for overall compression. Split F into $N \times N$ range blocks that do not overlap each other.

Step 2: In a window of $2N \times 2N$, a step size δ intercepts domain blocks along F . Shrink domain blocks and perform eight equidistant transformations.

Step 3: According to above method, domain blocks are classified and the corresponding class of range blocks is obtained.

Step 4: Take a range block R_i from the p -th class of range blocks, and take a domain block D_j from the p -th class of domain blocks. Calculate s and o according to (2) and (3), until all domain blocks in the p -th class are all searched, find the best matching block of range block R_i .

Step 5: All range domain classes are matched with their corresponding domain block classes, and fractal codes of continuous m layer image is obtained.

C. RESIDUAL COMPENSATION MECHANISM

Since the reconstructed image after lossy compression retains most of information for the original image, it is considered that there is a strong correlation between the reconstructed image and the original image. Residual image of the original image and the reconstructed image is not random noise. This conclusion has direct guiding significance for the following coding. Eq.6 gives the basic formula for calculating residual image in this paper.

$$r(x, y) = f(x, y) - g(x, y) \quad (6)$$

where $r(x, y)$ is the pixel value of the residual image, $f(x, y)$ is the pixel value of the original image, and $g(x, y)$ is the pixel value of the reconstructed image.

Residual image of the reconstructed image is obtained after the original image is greatly compressed, and corresponding ROI region is found on the residual image. A Huffman coding based on an integer squared quantization threshold is performed on the region with a finer threshold. The obtained code stream data is transmitted along with the original coded data, thereby completing lossless coding of the ROI region under Huffman coding. The algorithm framework is shown in Fig. 4.

The following are specific steps of the residual compensation mechanism algorithm:

Input: Original image and reconstructed image.

Output: Residual code file.

Step 1: Calculate the residual image.

Step 2: Retain the important coefficient of the threshold under a certain quantization threshold and generate a basic image to find the ROI region of the remaining coefficient.

Step 3: Huffman coding encodes a finer integer squared quantization threshold for the ROI region.

Step 4: The obtained code stream data is transmitted following the original coded data.

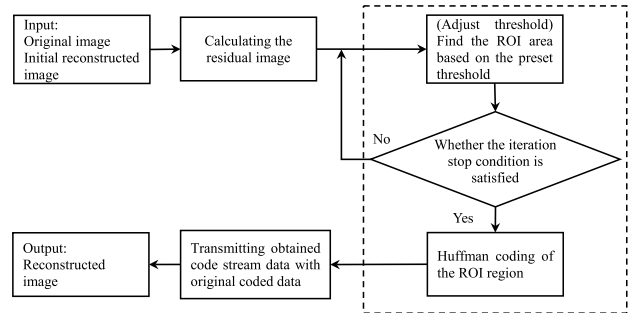


FIGURE 4. Flow chart of residual compensation mechanism.

TABLE 1. Information of ADNI data set.

Name	Description
Screening	Subjects who have a screening scan
Complete 1Yr	Subjects who all have screening, 6 and 12 month scans
Complete 2Yr	Subjects who have screening , 6 months, 1 year, 18 months and 2 year scans

IV. EXPERIMENTAL RESULTS AND ANALYSIS

Experiments are deployed on a computer with an Intel-Core i5-4590 CPU and a 12GB memory. The operating environment is Matlab2016a. MRI image sequences in the ADNI data set are taken as examples [35], and image size is $160 \times 192 \times 192$, 8 bits/pixel. Description of data set is shown in Table 1. We compare the proposed algorithm with traditional fractal MRI image compression algorithm from two aspects. They are a comparison of single-layer image compression and continuous layer image compression, respectively. In addition, the algorithm of this paper is compared with the BWT-MTF algorithm [36]–[37]. In these experiments, size of range block is selected as 4×4 , and size of domain block is 8×8 , and the horizontal step and the vertical step are both 8.

We evaluate quality of the decoded image by calculating PSNR by Eq.7. The peak signal-to-noise ratio (PSNR) is the logarithmic value of mean squared error (MSE) between the original image and the decoded image relative to $(2^n - 1)^2$, where $2^n - 1$ represents upper limit of gray level. n is the number of bits per pixel. The larger the PSNR value, the less distortion is represented. In addition, comparison indicators include compression time (T), speedup ratio (SR), and compression ratio (CR) by Eqs.7-9.

1) PEAK SIGNAL TO NOISE RATIO (PSNR) INDICATOR

$$\left\{ \begin{array}{l} PSNR = 10 \times \log_{10} \left[\frac{(2^8 - 1)^2}{MSE} \right] \\ MSE = \frac{1}{n} \sum_{i=1}^n (X_i - Y_i)^2 \end{array} \right. \quad (7)$$

where n is the number of pixels for the image. X_i and Y_i represent gradation values of the i -th pixel for images X and Y , respectively.

2) SPEEDUP RATIO (SR) INDICATOR

$$SR = \frac{T_S}{T_C} \quad (8)$$

where T_S is the time required to adopt traditional fractal MRI image compression method. T_C is the time required for the method in this paper.

3) COMPRESSION (SR) INDICATOR

$$CR = \frac{160 \times 192 \times 10}{H \times (8 + 8 + 3 + 8 + 3)} \quad (9)$$

where H is the number of range blocks. $\{8,8,3,8,3\}$ represents the quantization level of fractal parameters $\{x_i, y_i, t_i, s_i, o_i\}$, respectively, which is the memory required to save these parameters.

A. COMPARISON FOR CONTINUOUS LAYER OF MRI IMAGES

The first 4 layers of each MRI image are selected for compression. Calculate average compression time and PSNR for the 4 layers. The size of the original image slice is 160×192 , size of range block is 4×4 , and segmentation yields 40×48 range blocks. Size of domain block is defined as 8×8 , the horizontal step and the vertical step are both 8, and segmentation yields 20×24 domain blocks. According to the spatiotemporal similarity of image blocks, domain blocks are divided into 3 classes. Accordingly, range blocks are also divided into 3 classes. Table 2 is a restored image after compression and decompression of the first layer image for the three MRI images using the traditional fractal encoding algorithm and the proposed algorithm. Table 3 is experimental data [average T(s), average PSNR(dB)].

It can be seen from Table 2 and Table 3 that quality of the reconstructed image obtained by traditional algorithm and proposed is not much different observed by the human eye, which indicates that the algorithm is feasible. Secondly, compared with the traditional fractal coding algorithm, PSNR value is slightly reduced, but coding time is significantly shortened. This is because the traditional method uses global search, and the method first classifies all image blocks. As mentioned above, all range and domain blocks are divided into 3 classes. In theory, the speed should be up to three times. However, due to the non-uniformity of the classification, the actual acceleration is less than three times.

B. COMPARISON FOR MRI IMAGES WITH RESIDUAL COMPENSATION MECHANISM

We compress the first 4 layers of the three MRI images. A combination strategy is used that combines the four layers of images together and compresses them. Classification of domain blocks and range blocks is also done globally.

TABLE 2. Comparison for decoding quality of traditional algorithm and proposed algorithm.

Image Name	Screening	Complete 1Yr	Complete 2Yr
Uncompressed			
Traditional fractal coding algorithm			
The proposed algorithm			

TABLE 3. Comparison for performance of traditional algorithm and proposed algorithm.

Method	Screening		Complete 1Yr		Complete 2Yr	
	T	PSNR	T	PSNR	T	PSNR
Traditional	29.04	27.24	29.29	28.27	29.06	29.96
Proposed	11.25	26.68	10.55	27.52	10.25	29.15

The “codebook” is expanded from a single layer image to a 4-layer image, effectively improving matching accuracy. We first compress the 4-layer image without residual compensation mechanism, then compress it using the improved fractal coding method with residual compensation mechanism. After combining, domain blocks and range block are divided into corresponding 10 classes. Table 4 is a performance comparison of the three methods, where PSNR is the average of the 4-layer image.

It can be seen from Table 4 and Table 5 that the image quality obtained by the proposed algorithms with residual compensation mechanism is optimal. Although its compression time is higher than the the proposed algorithms without residual compensation mechanism, it is still much smaller than the time required by traditional method, and its PSNR is also the highest of the three. When four layers of MRI images are combined and compressed together, the time is four times that of a single layer image. But at this time all range and domain blocks are divided into 10 classes, so there is still speed-up effect. The compression time is 2.5 times that of traditional method. In addition, the introduction of RCM significantly improves quality of reconstructed images. It should effectively compensate for the error loss.

C. COMPARISON BETWEEN THE PROPOSED ALGORITHM AND BWT-MTF ALGORITHM

The BWT-MTF algorithm is a medical image compression model that implements efficient transmission of medical images using Huffman coding and hybrid fractal coding block

TABLE 4. Comparison for decoding quality of three algorithms.

Image Name	Screening	Complete 1Yr	Complete 2Yr
Uncompressed			
Without residual compensation mechanism			
With residual compensation mechanism			

TABLE 5. Performanc comparison for different strategies of the algorithm.

Method	Screening		Complete 1Yr		Complete 2Yr	
	T	PSNR	T	PSNR	T	PSNR
Traditional	116.16	27.24	117.16	28.27	116.24	29.96
Without RCM	45.00	26.68	42.20	27.52	41.00	29.15
With RCM	47.23	36.83	48.43	37.90	50.26	39.82

TABLE 6. Comparison of decoding quality for the proposed algorithm and BWT-MTF algorithm.

Image Name	Screening	Complete 1Yr	Complete 2Yr
Uncompressed			
The proposed algorithm			
The BWT-MTF algorithm			

BWT-MTF. In this method, a block-based Burrows-Wheeler compression algorithm is used to separate the regions containing the most needed diagnostic features and then encoded without significant loss in diagnostic quality. The remaining regions are encoded using a hybrid fractal coding algorithm. Finally, the two coding regions are combined to reconstruct the output image. Table 6 and Table 7 are comparison data of decoding quality and performance for the algorithm in the paper and the BWT-MTF method, respectively. PSNR is the average value of all the images included in each MRI medical

TABLE 7. Performance comparison for the proposed algorithm and BWT-MTF algorithm.

Name	Method	T	PSNR	CR	SR
Screening	Proposed	2276	40.42	3.75	2.46
	BWT-MTF	1075	34.56	4.20	
Complete 1Yr	Proposed	2314	40.64	4.79	2.42
	BWT-MTF	1021	35.32	4.45	
Complete 2Yr	Proposed	2427	45.70	4.13	2.31
	BWT-MTF	940	38.35	4.58	

image. Since each MRI image contains 192 layers, the time is the total compression time.

As can be seen from Tables 6 and 7, compression ratio of Screening and Complete 2Yr are reduced compared to the BWT-MTF algorithm, but their PSNR are significantly improved. Compression ratios of Complete 1Yr is higher than that of BWT-MTF algorithm. PSNRs of the three MRI images are higher than the BWT-MTF algorithm. Unfortunately, compression time of proposed method is greater than the BWT-MTF algorithm. This is a flaw of fractal compression algorithm. Compared to traditional algorithm, compression speed is increased by about 2 to 3 times. Since classification of range blocks and domain blocks is not uniform, it causes a difference between actual acceleration and theoretical acceleration.

V. CONCLUSION

With the rapid development of medical imaging technology, a large number of three-dimensional medical data, such as MRI, CT and three-dimensional ultrasound, have been produced. The volume of three-dimensional medical image data is large, resulting in high storage and transmission costs of network traffic during diagnostics and treatment. Proper compression of medical images reduces the amount of data transferred. Compressed data is then stored and transmitted. It not only saves storage space, but also improves transmission efficiency and shortens transmission time during remote diagnosis. Thereby promoting the development of medical care. In addition to retaining important information in medical images, increasing the compression ratio and decoding ability of compressed images is a major problem in medical image compression.

In response to the above problems, we propose a fast MRI image compression method based on fractal. First, three-dimensional MRI image is converted into two-dimensional sequence image. The sequence image-based fractal compression method is used to compress it. Secondly, range blocks and domain blocks are classified according to the spatiotemporal similarity feature. A range block only needs to search for the optimal matching block in a certain type of domain block. Accelerate by reducing the capacity of matching pool. Finally, a residual compensation mechanism

is introduced to achieve approximate lossless compression of MRI images. The experimental results show that compared with the traditional fractal MRI image compression method, the proposed method significantly improves compression speed when image quality is similar. Compared with the BWT-MTF algorithm, although compression ratio is sometimes slightly worse, the PSNR is higher than BWT-MTF. Validity of the proposed method is verified.

In the future, we need to improve works as follows. 1) consider to recruit more subjects in our future studies and perform statistical test; 2) further construct new features to enhance the definition of domain partition classification; 3) based on cloud computing, deep learning and other concepts, propose a more effective medical image compression algorithm; 4) start from the compression algorithm itself for improving its resistance to error.

REFERENCES

- [1] A. Bruckmann and A. Uhl, "Selective medical image compression techniques for telemedical and archiving applications," *Comput. Biol. Med.*, vol. 30, pp. 153–169, 2000.
- [2] P. G. Tahoces, J. R. Varela, M. J. Lado, and M. Souto, "Image compression: Maxshift ROI encoding options in JPEG2000," *Comput. Vis. Image Understand.*, vol. 109, pp. 139–145, Feb. 2008.
- [3] Y.-D. Zhang, Z. Dong, L. Wu, and S. Wang, "A hybrid method for MRI brain image classification," *Expert Syst. Appl.*, vol. 38, pp. 10049–10053, Aug. 2011.
- [4] S. M. Hosseini and A.-R. Naghsh-Nilchi, "Medical ultrasound image compression using contextual vector quantization," *Comput. Biol. Med.*, vol. 42, pp. 743–750, Jul. 2012.
- [5] P. E. Sophia and J. Anitha, "Implementation of region based medical image compression for telemedicine application," in *Proc. IEEE Int. Conf. Comput. Intell. Comput. Res.*, Dec. 2014, pp. 1–4.
- [6] M. Kaur and V. Wasson, "ROI based medical image compression for telemedicine application," *Procedia Comput. Sci.*, vol. 70, pp. 579–585, Dec. 2015.
- [7] P. Schelkens, A. Munteanu, and J. Cornelis, "Wavelet-based compression of medical images: Protocols to improve resolution and quality scalability and region-of-interest coding," *Future Gener. Comput. Syst.*, vol. 15, no. 2, pp. 171–184, 1999.
- [8] K. V. Sridhar, "Implementation of prioritised ROI coding for medical image archiving using JPEG2000," in *Proc. Int. Conf. Signals Electron. Syst.*, Sep. 2008, pp. 239–242.
- [9] M. Hu, C. Zhang, J. Lu, and B. Zhou, "A multi-ROIs medical image compression algorithm with edge feature preserving," in *Proc. 3rd Int. Conf. Intell. Syst. Knowl. Eng.*, Nov. 2008, pp. 1075–1080.
- [10] M. Firoozbakht et al., "Compression of digital medical images based on multiple regions of interest," in *Proc. 4th Int. Conf. Digit. Soc.*, Feb. 2010, pp. 260–263.
- [11] J. Bartrina-Rapesta, J. Serra-Sagristà, and F. Aulí-Llinàs, "JPEG2000 ROI coding through component priority for digital mammography," *Comput. Vis. Image Understand.*, vol. 115, no. 1, pp. 59–68, Jan. 2011.
- [12] D. Agrafiotis, D. R. Bull, and N. Canagarajah, "Region of interest coding of volumetric medical images," in *Proc. Int. Conf. Image Process.*, Sep. 2003, p. III-217.
- [13] K. Wang and A. Cuhadar, "Unbalanced 3-D tree structure for region-based coding of volumetric medical images," in *Proc. IEEE Int. Conf. Eng. Med. Biol. Soc.*, Aug./Sep. 2006, pp. 3286–3289.
- [14] V. Sanchez, R. Abugharbieh, and P. Nasiopoulos, "3-D scalable medical image compression with optimized volume of interest coding," *IEEE Trans. Med. Imag.*, vol. 29, no. 10, pp. 1808–1820, Oct. 2010.
- [15] B. P. Nguyen, C.-K. Chui, S.-H. Ong, and S. Chang, "An efficient compression scheme for 4-D medical images using hierarchical vector quantization and motion compensation," *Comput. Biol. Med.*, vol. 41, pp. 843–856, Sep. 2011.
- [16] V. Sanchez, "Joint source/channel coding for prioritized wireless transmission of multiple 3-D regions of interest in 3-D medical imaging data," *IEEE Trans. Biomed. Eng.*, vol. 60, no. 2, pp. 397–405, Feb. 2013.
- [17] E. S. Ahmed, N. Benamrane, and A. Taleb-Ahmed, "Adaptive medical image compression based on lossy and lossless embedded zerotree methods," *J. Inf. Process. Syst.*, vol. 13, no. 1, pp. 40–56, 2017.
- [18] D. Yee, S. Soltaninejad, D. Hazarika, G. Mbuyi, R. Barnwal, and A. Basu, "Medical image compression based on region of interest using better portable graphics (BPG)," in *Proc. IEEE Int. Conf. Syst.*, Oct. 2017, pp. 216–221.
- [19] K. V. Sridhar and K. S. R. K. Prasad, "Medical image compression using advanced coding technique," in *Proc. 9th Int. Conf. Signal Process.*, Oct. 2008, pp. 2142–2145.
- [20] K. M. M. Prabhu, K. Sridhar, M. Mischi, and H. N. Bharath, "3-D warped discrete cosine transform for MRI image compression," *Biomed. Signal Process. Control.*, vol. 8, no. 1, pp. 50–58, 2013.
- [21] S. Bhavani and K. G. Thanushkodi, "Comparison of fractal coding methods for medical image compression," *IET Image Process.*, vol. 7, no. 7, pp. 686–693, Oct. 2013.
- [22] S. Juliet, E. B. Rajasingh, and K. Ezra, "A novel medical image compression using Ripplelet transform," *J. Real-Time Image Process.*, vol. 11, no. 2, pp. 401–412, 2016.
- [23] Y.-D. Zhang, Y. Jiang, W. Zhu, S. Lu, and G. Zhao, "Exploring a smart pathological brain detection method on pseudo Zernike moment," *Multimedia Tools Appl.*, vol. 77, pp. 22589–22604, Sep. 2018.
- [24] S. Juliet, E. B. Rajasingh, and K. Ezra, "A novel image compression method for medical images using geometrical regularity of image structure," *Signal Image Video Process.*, vol. 9, pp. 1691–1703, Oct. 2015.
- [25] U. V. S. G and R. Nadarajan, "A rapid compression technique for 4-D functional MRI images using data rearrangement and modified binary array techniques," *Australas. Phys. Eng. Sci. Med.*, vol. 38, no. 4, pp. 731–742, 2015.
- [26] Y.-D. Zhang, K. Muhammad, and C. Tang, "Twelve-layer deep convolutional neural network with stochastic pooling for tea category classification on GPU platform," *Multimedia Tools Appl.*, vol. 77, no. 17, pp. 22821–22839, Sep. 2018.
- [27] S. Juliet, E. B. Rajasingh, and K. Ezra, "Projection-based medical image compression for telemedicine applications," *J. Digit. Imag.*, vol. 28, no. 2, pp. 146–159, 2015.
- [28] U. Patbhaje, R. Kumar, A. Kumar, and H.-N. Lee, "Compression of medical image using wavelet based sparsification and coding," in *Proc. 4th Int. Conf. Signal Process. Integr. Netw. (SPIN)*, Feb. 2017, pp. 394–398.
- [29] G. U. V. Selvi and R. Nadarajan, "CT and MRI image compression using wavelet-based contourlet transform and binary array technique," *J. Real-Time Image Process.*, vol. 13, no. 2, pp. 261–272, 2017.
- [30] K. C. Pathak and J. N. Sarvaiya, "Lossless medical image compression using transform domain adaptive prediction for telemedicine," in *Proc. Int. Conf. Wireless Commun., Signal Process. Netw. (WiSPNET)*, Mar. 2017, pp. 1026–1031.
- [31] H. Amri, A. Khalfallah, M. Gargouri, N. Nebhani, J.-C. Lapaire, and M.-S. Bouhlel, "Medical image compression approach based on image resizing, digital watermarking and lossless compression," *J. Signal Process. Syst.*, vol. 87, no. 2, pp. 203–214, 2017.
- [32] Y.-D. Zhang, C. Pan, X. Chen, and F. Wang, "Abnormal breast identification by nine-layer convolutional neural network with parametric rectified linear unit and rank-based stochastic pooling," *J. Comput. Sci.*, vol. 27, pp. 57–68, Jul. 2018.
- [33] S. Parikh, D. Ruiz, H. Kalva, G. Fernández-Escribano, and V. Adzic, "High bit-depth medical image compression with HEVC," *IEEE J. Biomed. Health Inform.*, vol. 22, no. 2, pp. 552–560, Mar. 2018.
- [34] X. W. Jiang, "Application of networking technology in special education," *J. Nanjing Tech. College Special Educ.*, vol. 4, pp. 5–7, Dec. 2012.
- [35] Alzheimer's Disease Neuroimaging Initiative. Accessed: Mar. 20, 2019. [Online]. Available: <http://adni.loni.usc.edu>
- [36] C. P. Devadoss and B. Sankaragomathi, "Near lossless medical image compression using block BWT-MTF and hybrid fractal compression techniques," *Cluster Computing*, 2018. doi: [10.1007/s10586-018-1801-3](https://doi.org/10.1007/s10586-018-1801-3).
- [37] X. Jiang, "Isolated Chinese sign language recognition using gray-level co-occurrence matrix and parameter-optimized medium Gaussian support vector machine," in *Proc. 7th Int. Conf. Frontiers Intell. Comput., Theory Appl. (FICTA)*, 2019, pp. 1–10.